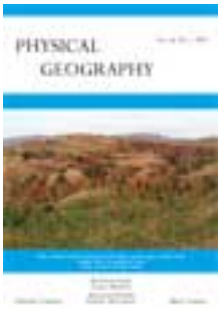

Physical Geography
Publication details, including instructions for authors and subscription information:
http://www.tandfonline.com/loi/tphy20

Cloud-to-ground lightning signatures of long-lived tornadic supercells on 27-28 April 2011

Stephen M. Strader[a] & Walker S. Ashley[a]
[a] Department of Geography, Northern Illinois University, Davis Hall Room 118, DeKalb, IL 60115, USA
Published online: 22 May 2014.

To cite this article: Stephen M. Strader & Walker S. Ashley (2014): Cloud-to-ground lightning signatures of long-lived tornadic supercells on 27-28 April 2011, Physical Geography

To link to this article: http://dx.doi.org/10.1080/02723646.2014.918527

Physical Geography, 2014
http://dx.doi.org/10.1080/02723646.2014.918527

Taylor & Francis
Taylor & Francis Group

Cloud-to-ground lightning signatures of long-lived tornadic supercells on 27–28 April 2011

Stephen M. Strader* and Walker S. Ashley

Department of Geography, Northern Illinois University, Davis Hall Room 118, DeKalb, IL 60115, USA

(*Received 19 February 2013; accepted 20 April 2014*)

This study integrates past research methodologies, data from the National Lightning Detection Network (NLDN), and geographic information system techniques to assess the lightning and severe weather hazard relationship for the 27–28 April 2011 United States tornado outbreak. NLDN and Doppler radar data are used to examine the cloud-to-ground (CG) lightning characteristics associated with seven supercell thunderstorms that produced long-track, significant and/or violent tornadoes. Analyses indicate that CG lightning flashes alone do not provide enough information for the detection of a lightning jump prior to tornadogenesis. All seven supercells were dominated by negative-polarity CG lightning flashes; which is expected due to the geographic location and elevated low-level moisture found in the outbreak environment. The correlation between low-level mesocyclone strength and total CG lightning flash rate was varied and inconsistent among all storms despite their formation and sustenance in similar environmental and geographic space. Additional case studies, as well as climatological approaches, are required to discover if the varying lightning–tornado relationships found in this study are consistent with other tornadic environments.

Keywords: supercells; tornadoes; cloud-to-ground; lightning; mesocyclone; geographic information systems; 27 April 2011

Introduction

Since the installation of the National Lightning Detection Network (NLDN) in the late 1980s, remotely sensed lightning attributes have been employed as useful nowcasting tools for deep, moist convection (Cope, 2006; Kufa & Snow, 2006). Most notably, lightning characteristics and patterns associated with supercells, including those capable of producing tornadoes, have been examined extensively using a variety of research and geographical techniques. These methods include: relating updraft strengthening (weakening) to the production of convective hazards that include tornadoes, large hail, and downbursts (McKinney, Carey, & Patrick, 2009; Murphy & Demetriades, 2005); analyzing a supercell's charge structure and the surrounding environment's role on modifying a supercell's charge structure (Smith, LaDue, & MacGorman, 2000); and assessing lightning flash rates in relation to the timing of tornadogenesis (Bluestein & MacGorman, 1998; Carey, Petersen, & Rutledge, 2003; Knapp, 1994; Knupp, Paech, & Goodman, 2003; MacGorman & Burgess, 1994; McCaul, Buechler, Hodanish, & Goodman, 2002; McDonald, McCarthy, & Patrick, 2006; McKinney et al., 2009; Perez, Wicker, & Orville,

*Corresponding author. Email: sstrader@niu.edu

1997; Schultz, Petersen, & Carey, 2009; Seimon, 1993; Steiger, Orville, Murphy, & Demetriades, 2005). Many of these studies contend that the timing of tornadogenesis and lightning flash rate relationship could potentially provide a tool for operational forecasters that would allow them to better predict tornadogenesis, increase lead time, and ultimately save lives (Cope, 2006; Kufa & Snow, 2006).

This study integrates past research methodologies along with unique geographic information system (GIS) techniques to analyze the cloud-to-ground (CG) lightning and severe weather hazard relationship for the 27–28 April 2011 United States tornado outbreak. Data from the NLDN are used to examine the lightning characteristics associated with seven supercell thunderstorms (11 tornado events) that produced long-track, significant, and/or violent tornadoes. Statistical and graphical analyses are used to determine how each tornadic supercell's total CG lightning flash rate varied throughout its life cycle, and evaluate the strength of the relationship between total CG lightning flash rate and low-level mesocyclone intensity.

Lightning and severe weather hazard relationship

A number of researchers have examined lightning flash rates in relation to severe weather hazards; ultimately, a wide range of conclusions in the literature have been presented. For instance, Seimon (1993), Knapp (1994), Perez et al. (1997), and McDonald et al. (2006) found that tornadogenesis had a tendency to occur during times of decreased, or time-series minimum in, CG lightning flashes. Past research has also concluded that there is a propensity for a rapid increase in total lightning flash rate when large hail is reported (Changnon, 1992; Knupp et al., 2003; Lang & Rutledge, 2005; MacGorman & Burgess, 1994; McCaul et al., 2002; McKinney et al., 2009; Shafer, MacGorman, & Carr, 2000). Others have observed similar results to those who analyzed the lightning–hail or lightning–tornado relationships with severe downburst events; their results suggest that the total lightning flash rate increased rapidly to its maximum value and was followed by a rapid decrease in total lightning flash rate in the moments prior to the wind event (Martinez & Schroeder, 2004; Seimon, 1993). Numerous studies (e.g., Deierling & Petersen, 2008; Kuhlman, Ziegler, Mansell, MacGorman, & Straka, 2006; Lang & Rutledge, 2002; Schultz et al., 2009; Wiens, Rutledge, & Tessendorf, 2005) have illustrated the relationship between updraft intensity in severe thunderstorms and lightning flash rates. More recently, total lightning activity (CG plus intracloud) detected using the NLDN and a local lightning mapping array (LMA) has proven useful in uncovering "lightning jumps" (i.e., a rapid increase in lightning flash rate) prior to severe convective hazard production (Schultz et al., 2009, Schultz, Petersen, & Carey, 2011). Greater updraft volumes and speeds are highly correlated ($r \geq 0.8$) to amplified lightning flash rate intensity because of the increased hydrometeor concentrations in the mixed ice-phase region (Deierling & Petersen, 2008). The elevated concentrations of hydrometeors in this region of a storm leads to a higher number of collisions between graupel and ice crystals, ultimately promoting greater charge separation and increased lighting activity (Deierling & Petersen, 2008). Thus, it is surmised that, given the strong ($>40\,\mathrm{ms}^{-1}$; Knupp et al., 2013) updraft velocities of the supercells on 27 April 2011, a relationship between lightning flash rates and updraft (mesocyclone) intensity and, ultimately, tornado production would be expected. Moreover, like Steiger et al. (2005) and Kufa and Snow (2006), we contend that, to understand fully the lightning and severe convective hazard

relationship, there needs to be a more comprehensive detailed approach to analyzing these severe weather events and their associated lightning attributes.

Data and methodology

NLDN

The United States has the largest network of lightning detection instruments in the world due to cooperation among government, private, and university sectors (Orville, 2008). The NLDN was the first lightning detection network implemented for the contiguous United States. The system was placed into operation in the late 1970s and early 1980s and underwent considerable expansion during the late 1980s. The installation of a lightning detection network permitted research into improving the understanding of the spatial distribution and density of total lightning flashes and thunderstorms across the contiguous United States (Orville, 2008).

A "total lightning" product, which is created by using the NLDN in combination with data derived from an LMA, appears more efficient at the detection of lightning jumps prior to tornadogenesis in comparison to utilizing CG data solely (Schultz et al., 2009, 2011); however, current LMAs are not, at this time, intended for operational use, restricting their suitability for real-time warning operations (Hodanish, Williams, & Boldi, 2013). Further, the spatial extent of LMA networks – e.g., the North Alabama LMA (NALMA), Washington DC LMA (DCLMA), Oklahoma LMA (OKLMA), and Kennedy Space Center LMA (KSC LDAR) – are limited and do not provide complete contiguous, or even regional, United States coverage. Hence, converse to the NLDN, LMAs provide limited applicability for present-day operational forecasting situations due to their restricted spatial coverage and operational usage status. While some of the supercells examined in this particular study did occur within the NALMA domain, the NALMA did not provide complete coverage for the southern and westernmost storms evaluated. Furthermore, many supercell lightning attributes were not available for NALMA-based analysis due to widespread power outages caused by the long-lived outbreak impacting the region (Carcione & Stano, 2012; NOAA, 2011). The primary motivation for this research was to determine if CG lightning data from the NLDN, which is operationally available, can be used solely in such an extreme severe weather situation to effectively analyze lightning flash rate characteristics and signals.

Employing similar statistical methods used for the detection of lightning jumps with total lightning data (i.e., time rate of change of the total flash rate thresholds; Schultz et al., 2009, 2011) is not valid when using CG lightning flash data from ground-based sensors solely (Ronald L. Holle, personal communication, 2012). CG lightning flash rates only represent a relatively small portion of the total lightning flash rates associated with a particular storm. Yet, it is possible that total CG lightning flash rates may be a proportional indicator of total lightning activity, thus providing useful information on the total lightning flash rate and tornadogenesis relationship (Ronald L. Holle, personal communication, 2012).

For this investigation, a lightning flash (CG lightning flash) is defined as the natural occurrence of electric discharge of very short duration and high voltage (that comes into contact with the ground) (Glickman, 2000; MacGorman, 1993; Schultz et al., 2009). For each flash, the NLDN data-set includes location (latitude and longitude), time (milliseconds), peak flash polarity (+ or −), amplitude (kiloamp (kA)), multiplicity, and error ellipse values (km). In 2011, the NLDN had a self-reported (Cummins &

Murphy, 2009) lightning detection efficiency of 99%, a flash detection efficiency of 95%, and a median location accuracy of 250–500 m. Variations in total flash density, positive flash density, percent positive, first stroke peak currents for both polarities, and multiplicity for both polarities seem to be influenced by topography (e.g., elevated terrain (Kotroni & Lagouvardos, 2008) and large bodies of water).

April 2011 severe weather event overview and methodology

During April 2011, more than 600 tornadoes were documented in the United States, making it the most active month for reported tornadoes on record (NOAA, 2011). Over 180 tornadoes were recorded during the 24-h period between 12:00 UTC 27 April and 12:00 UTC 28 April 2011 (NOAA, 2011). A total of 316 fatalities across six states were reported with the 27 April 2011 tornado outbreak, making it the second-deadliest day for tornadoes since record keeping began at the National Oceanic and Atmospheric Administration (NOAA, 2011). Overall, the 27 April 2011 tornado outbreak was one of deadliest and most destructive weather events in United States history.

For this investigation, seven long-lived, tornadic supercells (EF-3 or greater peak damage rating and damage paths of 32 km or longer) that occurred during the timeframe of 12:00 UTC 27 April to 12:00 UTC 28 April 2011 are examined using the NLDN and Doppler radar data from the National Climatic Data Center's (NCDC) radar archive (Table 1; Figure 1). Employing spatiotemporal methodologies, we present a comprehensive and controlled examination of the CG lightning flash–tornado relationship of long-lived tornadic supercells that developed, matured, and evolved in an environment and geographic region with similar kinematic and thermodynamic ingredients (i.e., low-level moisture values, storm relative helicity, convective available potential energy).

This study is the first to analyze the CG lightning–tornado relationship for such a violent severe weather outbreak. Similar to past studies, this research contends that lightning flash rates, in conjunction with radar observations and other forms of mesoanalysis, may be useful to understand better severe thunderstorm dynamics and evolution (e.g., Carey & Rutledge, 1998; Harlin et al., 2000; Kufa & Snow, 2006; MacGorman et al., 1989; Steiger et al., 2005).

Data processing involved three main tasks: (1) concatenating and placing the NLDN data into five-min lightning data bins, (2) converting the Doppler radar reflectivity data to shapefile format, and (3) combining and mapping CG lightning and radar reflectivity data using GIS software. All +CG lightning flashes from 0.1 to 10 kA were removed from the analysis because they are likely indicative of cloud discharges (Bentley & Stallins, 2005; Cummins et al., 1998; Wacker & Orville, 1999). The filtering of lightning flashes from 0.1 to 10 kA is attributable to the upgrade in the minimum waveform width criterion that was implemented to detect large, long-duration cloud pulses but, in turn, led to the misclassification of these large, long-duration intracloud (IC), cloud-to-cloud (CC), or cloud-to-air (CA) lightning pulses as weak CG flashes (Cummins et al., 1998). Evidence of this issue can be observed when examining peak currents of +CG flashes for both 1994 (pre-NLDN upgrade) and 1995 (post-NLDN upgrade) where the 1995 +CG flash detection counts were two times greater than those of the 1994 + CG counts' (Cummins et al., 1998). Though Cummins et al. (1998) suggest that the NLDN lightning sensor instrumentation upgrade, as opposed to instrumentation error, is responsible for the difference between 1994 and 1995 weak −CG

Table 1. Summary of the NWS survey results for tornadoes produced by the seven supercells examined in this study.

Storm	Tornado location	Tornado event	Peak damage rating	Path length (km)	Tornadogenesis (UTC)	Tornado dissipation (UTC)
A	*Mississippi* – Smithville; Chickasaw county *Alabama*-Shottsville	A-1	EF-5	111.7	20:04	21:20
B	*Alabama* – Hackleburg; Franklin, Lawrence. Morgan, Limestone, Madison counties	B-1	EF-5	212.5	20:05	22:20
C	*Mississippi* – Neshoba, Kemper, Winston, Noxubee counties	C-1	EF-5	46.7	19:30	20:00
	Alabama – Cordova; Pickens, Tuscaloosa, Fayette, Walker, Blount counties	C-2	EF-4	187.4	20:40	22:50
	Alabama – DeKalb county	C-3	EF-5	54.4	23:19	23:56
	Georgia – Catoosa county *Tennessee* – Hamilton county	C-4	EF-4	80.5	00:15	01:02
D	Tuscaloosa, AL Birmingham, AL	D-1	EF-4	129.8	21:43	23:14
	Alabama – Jefferson, St. Clair, Calhoun, Etowah, Cherokee counties	D-2	EF-4	114.7	23:28	24:47
E	*Alabama* – Greene, Hale, Bibb counties	E-1	EF-3	116	22:30	23:55
F	*Mississippi* – Smith, Jasper, Clarke counties *Alabama* – Choctaw county	F-1	EF-4	148.5	22:42	01:40
G	*Alabama* – Elmore, Tallapoosa, Chambers counties	G-1	EF-4	71.1	01:12	02:09

detection counts, −CG lightning flashes from −10 to −0.01 kA were removed to avoid any possible misclassification of IC, CC, CA flashes as CG lightning flashes.

Using methodologies similar to those used by Perez et al. (1997), Carey et al. (2003), and Knupp et al. (2003), lightning data were separated into five-min intervals or bins (e.g., 00:00:00 UTC–04:59.99 UTC, 05:00.00 UTC–09:59.99 UTC, etc.; Figure 2). Five-minute time intervals were selected as an analysis metric since this temporal binning most accurately resolved the lightning flash rates in comparison to the 10- and 15-min time periods (Perez et al., 1997; Figure 2).

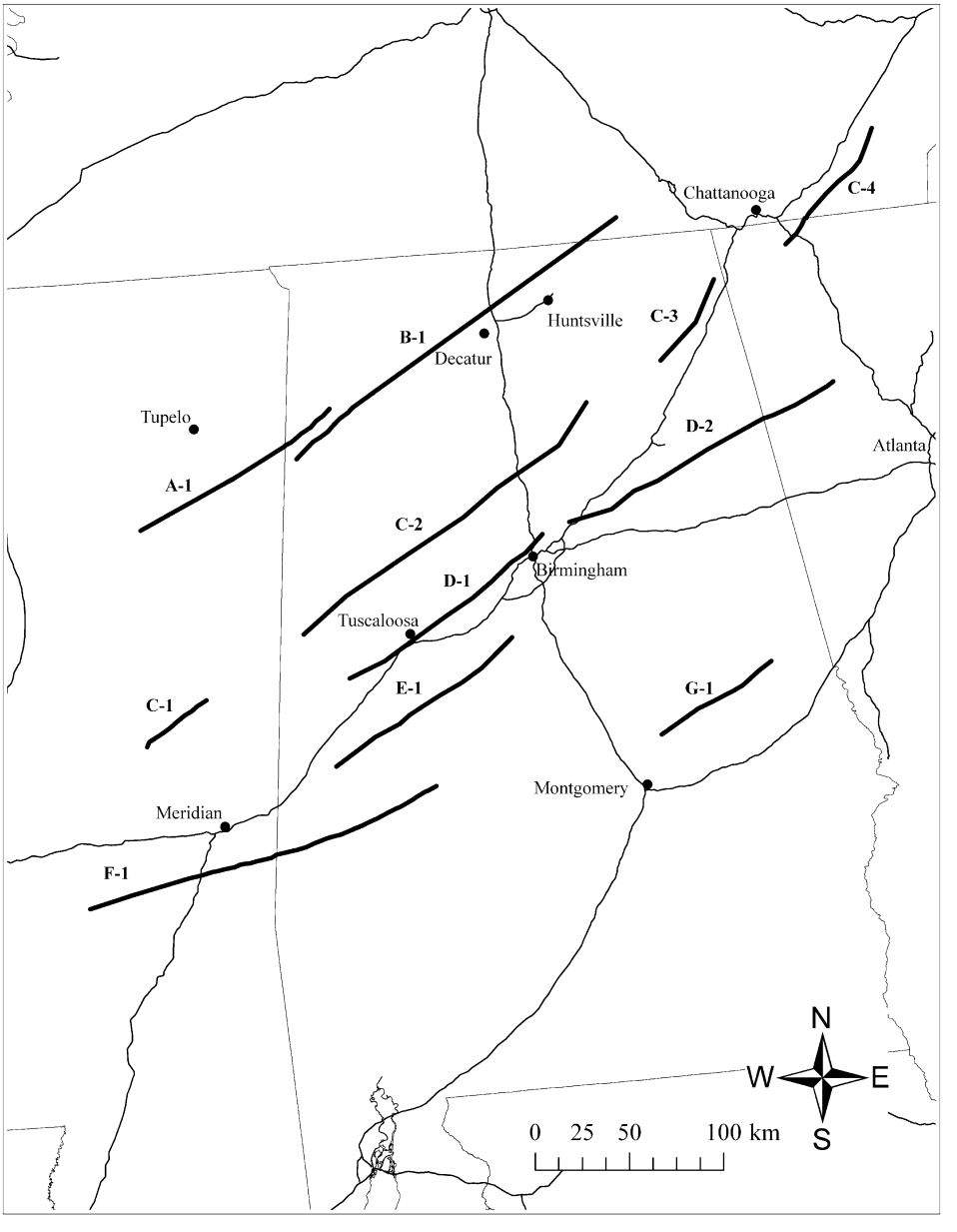

Figure 1. Paths of the tornadoes produced by the seven supercells examined.
Note: The letters represent the storms that were responsible for producing the tornadoes and the numbers represent the sequential order of the tornadoes produced by a particular storm throughout the severe weather event. (e.g., C-2 was the path of a tornado produced by Storm C and was the second tornado examined for supercell C within the research domain; cf. Table 1).

Though past studies analyzed lightning flash rates 30 min prior to tornadogenesis and 30 min following tornadolysis; for this particular study, each storm's initial lightning bin was created 15 min prior to the storm's first tornado report (e.g., a tornado is produced at 15:00 UTC, the initial lightning bin is then created for 00:00.00

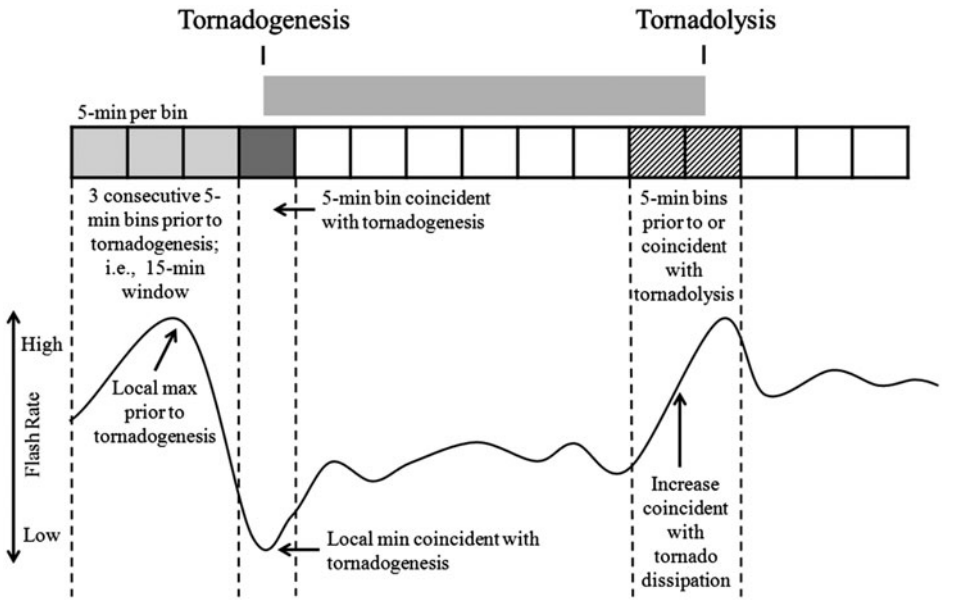

Figure 2. A conceptual model of the five-min lightning data binning scheme and hypothetical lightning flash rate for a tornadic storm based on previous literature (Perez et al., 1997). An example of a storm's lightning flash rate is overlaid to show how a local maximum prior to tornadogenesis, a local minimum coincident with tornadogenesis, and an increase coincident with tornado dissipation was evaluated.

UTC–04:59.99 UTC timeframe; Figure 2). This temporal restriction is attributable to the speed at which the storms were moving (23 m s^{-1} or greater) and the exceptionally rapid morphological evolution from convective initiation to isolated, unorganized cells, to supercell storm structure within the early stages of storm life cycle that typified this outbreak. As an example of this rapid evolution from isolated, unorganized cells to supercells, Storm B (Hackleburg, AL EF5) underwent rapid intensification from an isolated, unorganized cell (19:50.00 UTC) to producing a tornado (20:05.00 UTC) in 15–20 min. Similarly, each storm's final lightning data bin was created 15 min after the storm's final tornado had been produced (i.e., a tornado dissipates at 01:00 UTC then the final lightning bin is created for 01:10.00–01:14.99 UTC timeframe) (Figure 2). The initial lightning bin had its lowest bound rounded down to the nearest five-min integer if the tornado was not reported on a specific five-min integer (i.e., a tornado is reported at 32:00.00 UTC then the initial lightning bin is rounded down and created for the 10:00.00–14:59.99 UTC timeframe).

Manual and automated lightning determination methods

Properly determining, or matching, remotely sensed lightning flashes with their causative storm continues to be a challenge in lightning research (Kane, 1991, 1994; Perez et al., 1997). For this investigation, both a subjective and objective method was employed for CG lighting flash storm attribution.

First, a "lasso" method was used to determine and acquire the CG lightning flash data that are associated with each storm for every time stamp (Figure 3). The lasso

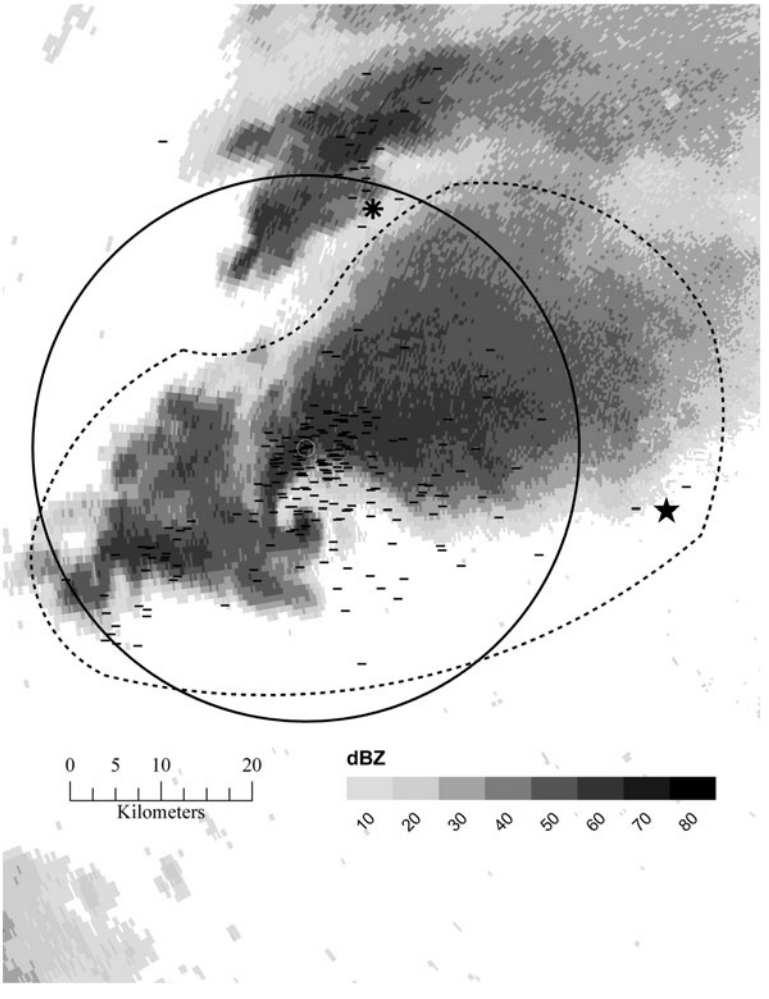

Figure 3. Example of objective (automated) buffer and manual lasso lightning selection methods for Storm D/Tornado D-1 (22:07.00 UTC through 22:12.99 UTC). The solid line illustrates the automated 30-km buffer being applied by selecting the storm center (highest reflectivity value); dashed line illustrates the manual lasso; the star and asterisk indicate areas of differentiation between the objective buffer and manual lasso methods discussed in the text.

method selects or encapsulates, clusters of the CG lightning flashes given Doppler radar base reflectivity imagery and the spatial extent of the storm. As in past research, a discrete or isolated thunderstorm is defined as 40 dBZ base reflectivity radar pixels adjacent to each other (Bentley, Stallins, & Ashley, 2012; Falconer, 1984; Parker & Knievel, 2005; Rickenbach & Rutledge, 1998). Determining the spatial extent of the 40 dBZ radar pixels adjacent to each other allowed for the separation and determination of the discrete, isolated storms. Once the storm's spatial extent was determined, a free-handed boundary (i.e., lasso) was used to select all CG lightning flashes and Doppler radar base reflectivity pixels associated with the storm (Figure 3). The selected CG lightning flashes were then used to represent the total CG lightning flashes associated with that storm over the given five-minute interval. The creation of a subjective,

user-defined lasso around a particular storm is desirable because of the non-uniform and/or inconsistent storm morphologies and characteristics (e.g., size, shape) associated with each case and the characteristics of the severe weather event (e.g., multiple long-lived supercells in close proximity to one another).

To compare the effectiveness of the manual lasso method, an objective (automated; fixed-distance) buffer method was also used. First, an objective buffer of 30 km was centered on the highest base reflectivity value for each reflectivity time stamp associated with a storm (Figure 3). Correspondingly, the CG lightning flash data associated with the five-min data bin that overlapped the reflectivity time stamp were overlaid on the radar data. The objective buffer then selected the CG lightning flashes within the 30-km radius, which were then used to represent the total CG lightning flashes for that particular storm over the five-min interval. All CG lightning flashes that fell within the 30-km automated buffer radius were presumed to be the CG lightning flashes associated with the storm. The buffer radius of 30 km was chosen since, based on assessments of a multitude of storms during the outbreak, that threshold appeared to most accurately encompass the individual storms and their associated CG lightning flashes.

Comparisons of the manual lasso and automated buffer methods illustrate that the manual lasso method performed better in determining the CG lightning flashes associated with a particular storm over a given five-minute interval (Table 2; e.g., Figure 3). As an illustration of this comparison, the automated buffer recorded a greater number of total CG lightning flashes throughout the life cycle of Storm D and included more CG lightning flashes (57), which is primarily due to the greater spatial extent of the automated buffer encompassing other discrete storms in close proximity (Table 2; Figure 3). For this storm, the automated buffer contained 55 more +CG lightning flashes than the manual lasso, which equates to a 9.6% difference (Table 2). Given the relatively rare occurrence of +CG lightning flashes for this severe weather event, a percent difference of 9.6% is noteworthy. The disparity in +CG lightning flash detection is likely due to a supercell's propensity to produce + CG lightning flashes in its forward-flank downdraft (FFD) region (Bruning, Rust, MacGorman, Biggerstaff, & Schuur, 2010).

While increasing the automated buffer, spatial extent could potentially better capture the + CG lightning flashes occurring in the FFD region of the supercell, it would also result in greater likelihood for the detection of CG lightning flashes associated with other discrete storms in close proximity (Figure 3; as indicated by the star and asterisk). Though the automated buffer had a sizeable spatial extent of 30 km and was centered on the highest radar reflectivity pixel of a particular storm of interest, it does not

Table 2. Storm D lightning counts from automated buffer and manual lasso methods. Values in bold indicate greater automated buffer difference metrics.

Metrics	Automated buffer	Manual lasso	Absolute difference	Percent difference
Total CG lightning flashes	10,553	10,496	57	0.5%
Total +CG lightning flashes	543	598	*55*	*9.6%*
Total −CG lightning flashes	10,010	9898	112	1.1%
Mean total lightning flash rate	47.97	46.80	–	–

always provide complete coverage of an isolated storm like a supercell which has tendencies to continually evolve and display complex morphological structure.

Whereas employing TITAN (Dixon & Wiener, 1993), SCIT (Johnson et al., 1998), and/or other storm-tracking algorithms allows for the employment of an objective lasso lightning flash selection method, these algorithms tend to suffer from false mergers, incorrect identification, tracking, and forecasting in cases where there are dense cells whose shape changes rapidly (cf. Figure 1 in Han et al., 2009). Though the manual lasso is variable in spatial extent and, by definition, requires subjective input, it is the optimal method for determining the 'natural' spatial breaks or clusters in CG lightning distribution associated with multiple storms in close proximity for small sample size studies.

Relationships between CG lightning flash rate, tornado life cycle, and mesocyclone strength

Time series analyses of total CG lightning flashes (both positive and negative polarities), total +CG lightning flashes, total −CG lightning flashes, time of tornadogenesis, duration of tornado, and time of tornadolysis were conducted throughout the life cycle of each of the seven storms in the study. These time series permitted statistical evaluations, such as percent difference, count, CG lightning flash rates, and measures of central tendency (mean), which were used to evaluate each storm/tornado event in comparison to the others. Further, they were used to assess if the following lightning hazard associations occurred: lightning maximum prior to tornadogenesis, local minimum coincident with tornado touchdown, an increase in total CG lightning flash rate coincident with tornadolysis, and/or a polarity shift coincident with tornado touchdown or during tornado production.

As in the work of Perez et al. (1997) and Gilmore and Wicker (2002), a local maximum in total CG lightning flash rate was defined as a peak in total CG lightning flash rate in the 15 min prior to tornadogenesis, whereas a local minimum in total CG lightning flash rate concurrent with tornadogenesis was defined as a minimum in total CG flash rate during the five-min lightning data bin that encompassed the time of touchdown (Figure 2). An increase in total CG lightning flash rate coincident with tornadolysis was defined as an increase in total CG lightning flash rate in the five min prior to tornado dissipation or during the 5-min lightning data bin that encompassed the time of tornado dissipation.

The low-level mesocyclone strength (measured from lowest elevation scan altitude to 4 km or, effectively, 0–4 km AGL) for a select number of tornado events (A-1, C-2, D-2, and E-1) within the research domain is examined and compared to their total CG lightning flash trends. Rotational velocity (V_r) and azimuthal (rotational) shear (S) were calculated and utilized to determine the strength of the low-level mesocyclone. As in the work of Stumpf et al. (1998), Atkins, Bouchard, Przybylinski, Trapp, and Schmocker (2005), and Wolf (2006), rotational velocity (V_r) was defined as

$$V_r = \frac{V_{\max} - V_{\min}}{2} \tag{1}$$

where $V_{\max}$ and $V_{\min}$ are the outbound and inbound storm-relative velocities, respectively. Also, as by Stumpf et al. (1998), azimuthal (rotational) shear (S) was defined as

$$S = \frac{V_r}{D} \tag{2}$$

where D is the distance between V_{max} and V_{min}. Due to Doppler radar coverage issues (i.e., power outages at National Weather Service facilities (Carcione & Stano, 2012; NOAA, 2011) and the radar beam's inability to sample the lowest 4 km of the storm, precluding information on the strength of the low-level mesocyclone) some storms within the research domain were excluded from this specific analysis. Once the rotational velocity and azimuthal (rotational) shear values were calculated, they were compared to total CG lightning flash rates throughout a specified time interval for a particular supercell investigated.

Results

Individual storm analysis: CG lightning flash rates and polarity

Of the seven tornadic supercells investigated in this study, all experienced mean total CG lightning flash rates greater than 11 flashes min^{-1} throughout their life cycles (Table 3). The percentage +CG lightning flashes was 7.5% for the seven supercells, which is much lower than the 22.9% found in Perez et al. (1997). Previous lightning climatology research (Mäkelä, Pecca, & Shultz, 2010; Orville, Huffines, Burrows, & Cummins, 2010) suggests that the geographic location and season of occurrence of this particular event may be the reason +CG lightning flashes were less common. Moreover, storms dominated by +CG flashes tend to occur in environments with drier low- to mid-level tropospheric air. As illustrated by Carey and Buffalo (2007), storms consisting of low (~32%) 700–500 hPa layer mean relative humidities, low (~14.2 °C) mean surface dew points, low (~10.9 g kg^{-1}) mean mixing ratios in the lowest 100 hPa of the troposphere, higher (~2080 m) mean lifted condensation levels (LCL), and low (~2.7 cm) precipitable water (PW) values from the surface to 400 hPa are more often dominated by +CG lightning flashes. Conversely, the supercells that occurred on 27 April 2011 formed in a favorable environment for the production of −CG lightning flashes (i.e., low-level dew point temperatures greater than 20 °C and PW values greater than 3.5 cm; accessed via 22:00 UTC BMX RUC storm proximity sounding and 22:00 UTC RUC model analysis) and contained storm characteristics commonly associated with the production of −CG lightning flashes (i.e., LCL heights less than 800 m; Carey & Buffalo, 2007). The storms assessed in this investigation had LCL heights of 400 m or less, which are appreciably low compared to typical LCL heights associated with non-tornado producing storms, non-significant tornado (EF2 or lower) producing storms, and pulse-style storms (Coleman, Knupp, & Murphy, 2012; Rasmussen & Blanchard, 1998).

In addition to lower than average LCL heights, the supercells in the outbreak exhibited higher than average freezing level (FL) heights. The lower than average LCL heights and higher than average FL heights resulted in a greater warm cloud depth (WCD), which can increase the efficiency of the relatively warm rain-collision-coalescence process and lead to greater −CG lightning flash rates (Carey & Buffalo, 2007; Rosenfeld & Woodley, 2003). Though previous research (Kotroni & Lagouvardos, 2008) has indicated terrain influences on lightning occurrence, we contend that terrain effects are negligible in these cases, given the intense updraft velocities and intensity which had a much greater influence on lightning flash rates.

As illustrated by Carey and Buffalo (2007), the mean WCD depths and FL heights for storms dominated by −CG lightning flashes are 2950 and 4070 m, respectively. Conversely, storms represented by a majority of +CG lightning flashes exhibited mean

Table 3. Lightning metrics for each storm (A-G) examined.

Storm	A	B	C	D	E	F	G
Total CG lightning flashes	1550	10,084	7860	10,496	2947	2315	3193
Total +CG flashes (kA)	93	780	434	598	237	183	203
Total −CG flashes (kA)	1457	9303	7425	9898	2710	2132	2990
Mean max. +CG stroke current (kA)	48.8	42.9	36.1	46.4	34.7	31.5	39.4
Mean max. −CG stroke current (kA)	−59.7	−78.7	−71.8	−106.6	−106.5	−80.4	−94.8
Percentage +CG flashes (%)	6.1	10.9	5.4	5.6	10.7	7.4	6.3
Mean average −CG flash pol. (kA)	−19.7	−19.2	−19.4	−20.8	−23.9	−24.5	−23.4
Mean average +CG flash pol. (kA)	32.2	21.7	23.3	23.0	22.00	22.9	24.5
Mean total CG flash rate (flash/min)	14.2	59.7	21.1	45.7	16.1	11.2	28.0

WCD depths and FL heights of 1700 m and 3780 m, respectively. The storms on 27–28 April 2011 were characterized by lower than average LCL heights (<400 m) and higher than average FL heights (>4500 m), which resulted in WCD of 4000 m or greater (accessed via 22:00 UTC BMX RUC analysis storm proximity sounding and 18:00 UTC BMX observed sounding). These environmental characteristics and storm features led to greater −CG lightning efficiency and, in turn, resulted in a much greater percentage of −CG flashes in comparison to +CG flashes. Overall, the supercells that occurred on 27–28 April 2011 were not only efficient producers of long-lived, long-tracked, violent tornadoes, but they also produced greater CG lightning flash rates in comparison to typical long-lived supercells assessed in prior research (Perez et al., 1997).

Of the seven supercells examined, Storm B (Hackleburg, AL) was the most prolific in terms of total CG lightning flash rate, exhibiting a mean total CG lightning flash rate of 59.7 flashes min^{-1} (Table 3). Storm B had the greatest mean total lightning flash rate because of its high liquid water, ice, and graupel content (i.e., it was a high-precipitation supercell) as well as ice particle seeding from the anvil of an upstream storm. Previous research has suggested that high liquid water, ice, and graupel content, as well as ice particle seeding from an upstream storm, can lead to greater total lightning flash rates (Brooks, Doswell, & Wilhelmson, 1994; Knupp et al., 2003; MacGorman & Burgess, 1994; Saunders, 1994). Seeding occurs when an upstream storm's anvil and downstream storm's mid-level precipitation processes interact (Knupp et al., 2003; Figure 4); in these cases, the upstream storm lofts small hail and graupel that is then carried downstream to the mid-levels of a downstream storm (Knupp et al., 2003). Generally, ice particle seeding occurs when the maximum reflectivity cores of two isolated storms are separated approximately 60–100 km from each other and their mid-to-upper level storm motions are similar (Knupp et al., 2003). In the case of Storm B (Figure 4), mid-to-upper level storm motions were analogous and the upstream storm's reflectivity core was 50–80 km from the core of Storm B, suggesting there was ice particle seeding occurring, which ultimately enhanced Storm B's precipitation efficiency and CG lightning production (Knupp et al., 2003).

Lightning and tornado relationship

Examining lightning patterns of multiple long-lived supercells is paramount to understanding the potential lightning–tornado relationship. In this section, the CG lightning attributes throughout the lifetimes of seven long-lived tornadic supercells (A-G) and 11 tornado events are assessed. Additionally, the low-level mesocyclone strength for a selected number of tornado events (A-1, C-2, D-2, and E-1) within the research domain is examined and compared to the total CG lightning flash trends associated with those tornadic events.

Employing the five-min lightning data binning scheme, a majority of storms (5 of 7) experienced a local maximum in total CG lightning flash rate *prior to* tornadogenesis. However, only tornado events A-1, B-1, C-2, C-3, and G-1 (5 of 11) have a local maximum using a three consecutive, five-min binning scheme (i.e., 15-min window; Table 4; Figures 2 and 5). Given the variability in timing of a total CG lightning flash maximum prior to tornadogenesis, the 15-min window provides the greatest confidence in capturing a local maximum in total CG lightning flashes prior to tornadogenesis as opposed to 10- or 5-min windows.

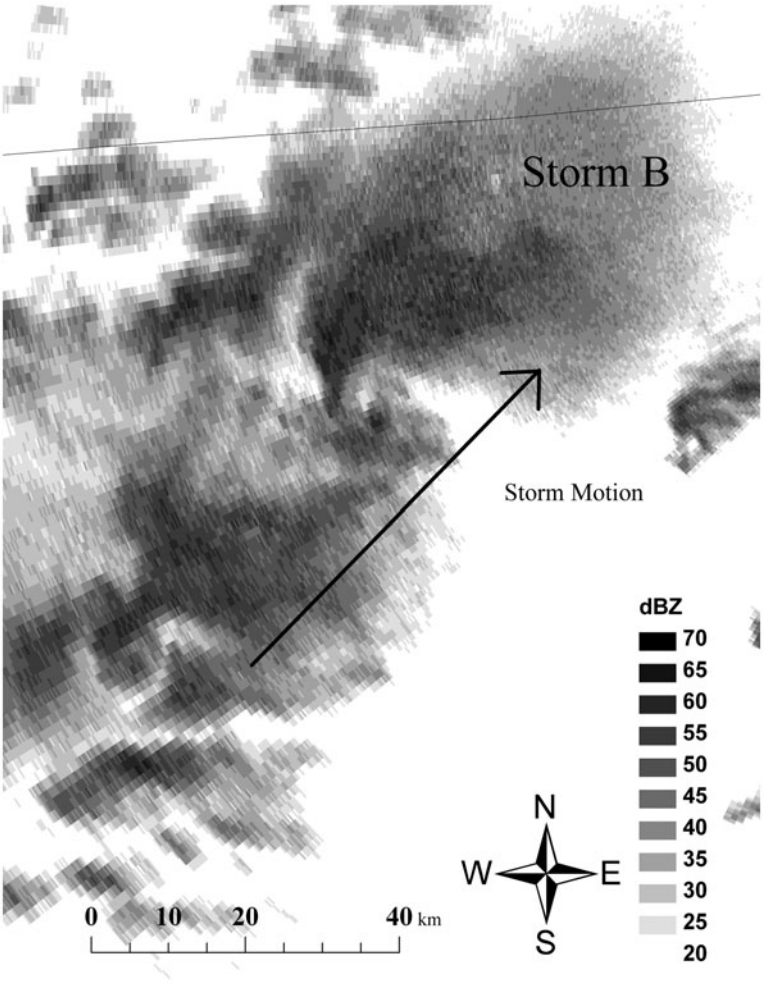

Figure 4. Doppler radar base reflectivity from KHTX at 21:15.58 UTC illustrating evidence of downstream–upstream storm ice particle seeding. The arrow represents the storms' directional motion.

While tornado events D-1 and E-1 initially appear to indicate a local maximum in total CG lightning flash rate prior to tornadogenesis, further analysis indicates that these events *did not* experience a local maximum in CG lightning flash rate (Figure 6). For both of these events, the local maximum in total CG lightning flash rates is a decline from a local maximum in total CG lightning flashes *preceding* the 15-min window prior to tornadogenesis. Given this uncertainty, tornado events D-1 and E-1 were recorded as having "not experienced" a local maximum in total CG lightning flash rate prior to tornadogenesis (Table 4). Further, tornado event D-2 did not experience a local maximum in total CG lightning flash rate in the 15-min window prior to tornadogenesis. Event D-2's local maximum in total CG lightning flash rate is concurrent with the increase in total CG lightning flash rate during tornado dissipation. Therefore, tornado D-2 was also recorded as having "not experienced" a local maximum in total CG lightning flash rate in the 15-min window prior to tornadogenesis.

Table 4. Lightning trends and attributes associated with each storm (A-G) employing the five-minute lightning data binning scheme (✓ indicates experienced and X indicates not experienced).

Storm	Tornado event	Local max. total CG flash rate prior to tornadogenesis (15-min window)	Local min. total CG flash rate coincident with tornadogenesis	Polarity shift coinciding with tornadogenesis or during tornado production	Increase in total CG flash rate coincident with tornado dissipation
A	A-1	✓	X	X	✓
B	B-1	✓	X	X	✓
C	C-1	X	X	X	X
	C-2	✓	✓	X	X
	C-3	✓	✓	X	✓
	C-4	X	X	X	✓
D	D-1	X	✓	X	✓
	D-2	X	X	X	✓
E	E-1	X	X	X	X
F	F-1	X	✓	X	X
G	G-1	✓	✓	X	✓

Using the five-min binning scheme, four of the seven supercells assessed contained a local minimum in total CG lightning flash rate *coincident with* tornadogenesis (Table 4; Figure 5). Yet, only 5 of 11 tornado events affiliated with these storms (C-2, C-3, D-1, F-1, and G-1) indicate a local minimum coincident with tornadogenesis (Table 4; Figure 5). To objectively test the relationship and statistical significance of a lightning jump prior to tornadogenesis, piecewise regression and spline regression modeling (with known knots) were employed (Marsh & Cormier, 2002; McDowall, McCleary, Meidinger, & Hay, 1980; Table 5). These tests permit the detection and evaluation of statistical significance of lightning jumps prior to tornadogenesis using total CG lightning flash rates. Tornado events A-1, C-2, D-2, and G-1 all illustrate statistically significant lightning jumps prior to tornadogenesis for at least the 90% confidence interval, while only tornado events A-1 and C-2 demonstrate statistically significant lightning jumps prior to tornadogenesis for all confidence intervals (90, 95, 99%; Table 5).

Four of the seven storms (A, B, D, and G) examined illustrate an increase in total CG lightning flash rates in the 5 min prior to or coincident with tornado dissipation. Tornado events A-1, B-1, C-3, C-4, D-1, D-2, and G-1 (7 of 11) had an increase in total CG lightning flash rates in the 5 min prior to or coincident with tornado dissipation (Table 4). While the five-minutes binning scheme indicates that 7 of 11 tornado events experience an increase in CG lightning flash rates, 9 of 11 tornado events indicate a decrease in total CG lightning flash rates in the five-min bin preceding the lightning bin coincident with tornadolysis. Thus, caution should be taken with these results as there is substantial variability in lightning flash trends during tornado dissipation.

Contrary to the results of Perez et al. (1997) and (Martinez and Schroder, 2004), none of the supercells presented in this investigation experienced a polarity shift that occurred prior to tornadogenesis, or simultaneously with tornadogenesis (Table 4). The lack of storms experiencing a polarity shift can be attributed to the time of year and location of the of the severe weather event (e.g., early spring, Southeast United States), as well as the moisture characteristics of the storms (i.e., the high dew point temperatures, high

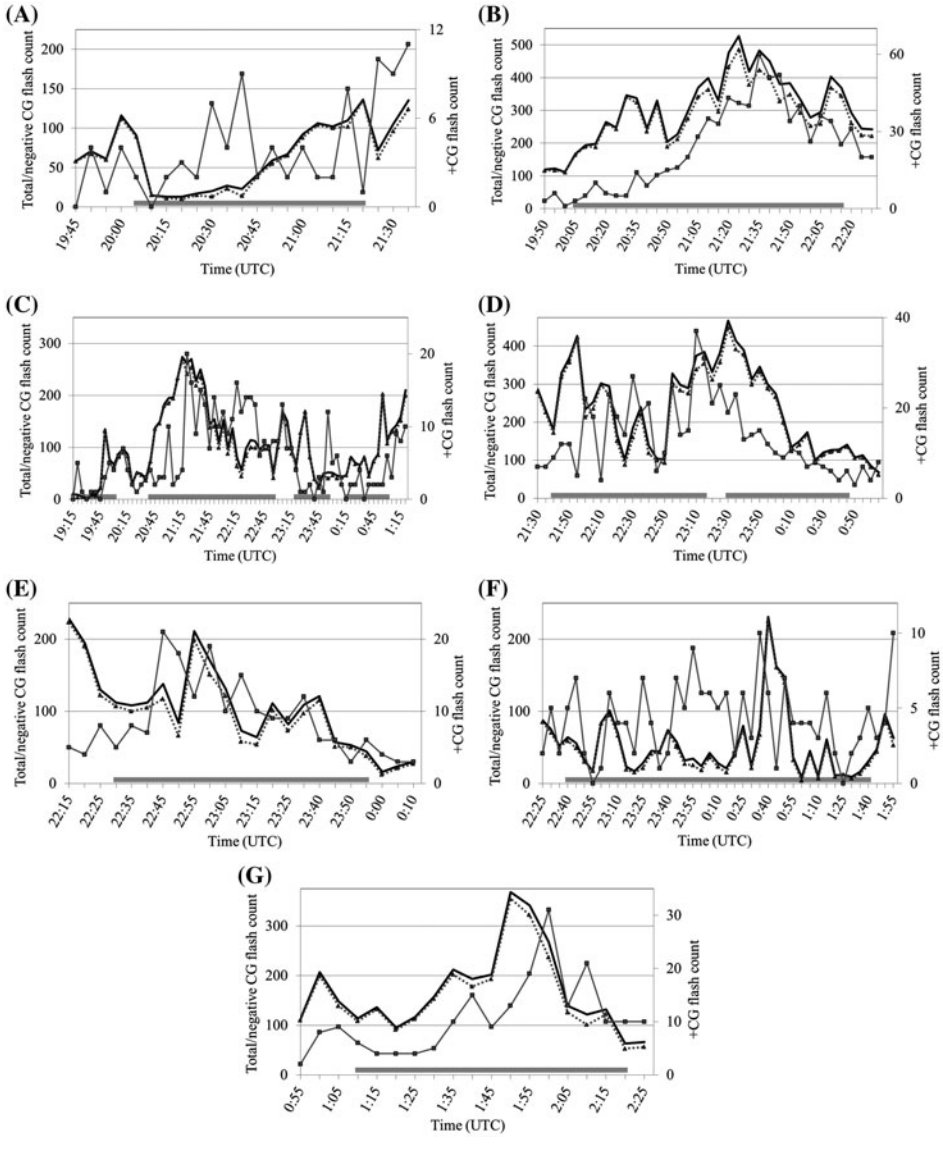

Figure 5. Temporal lightning trend analysis for Storms A-G.
Notes: Thick black lines indicate total CG flashes; gray lines with the triangle marker illustrate total −CG flashes; gray lines with the square marker represent the total +CG flashes; thick gray lines with no marker represent the duration of the tornado (cf. Table 1).

precipitable water values, and low LCL heights; Carey & Buffalo, 2007; Mäkelä et al., 2010; Orville et al., 2010). The majority of storms that commonly experience a polarity shift typically comprise a majority of +CG lightning flashes during the early stages of the thunderstorm life cycle (Carey & Buffalo, 2007; MacGorman & Burgess, 1994; Perez et al., 1997; Seimon, 1993; Smith et al., 2000).

All storms examined in this investigation formed in a region of weak surface equivalent potential temperature (θ_e) gradient and east of a surface θ_e maximum which likely

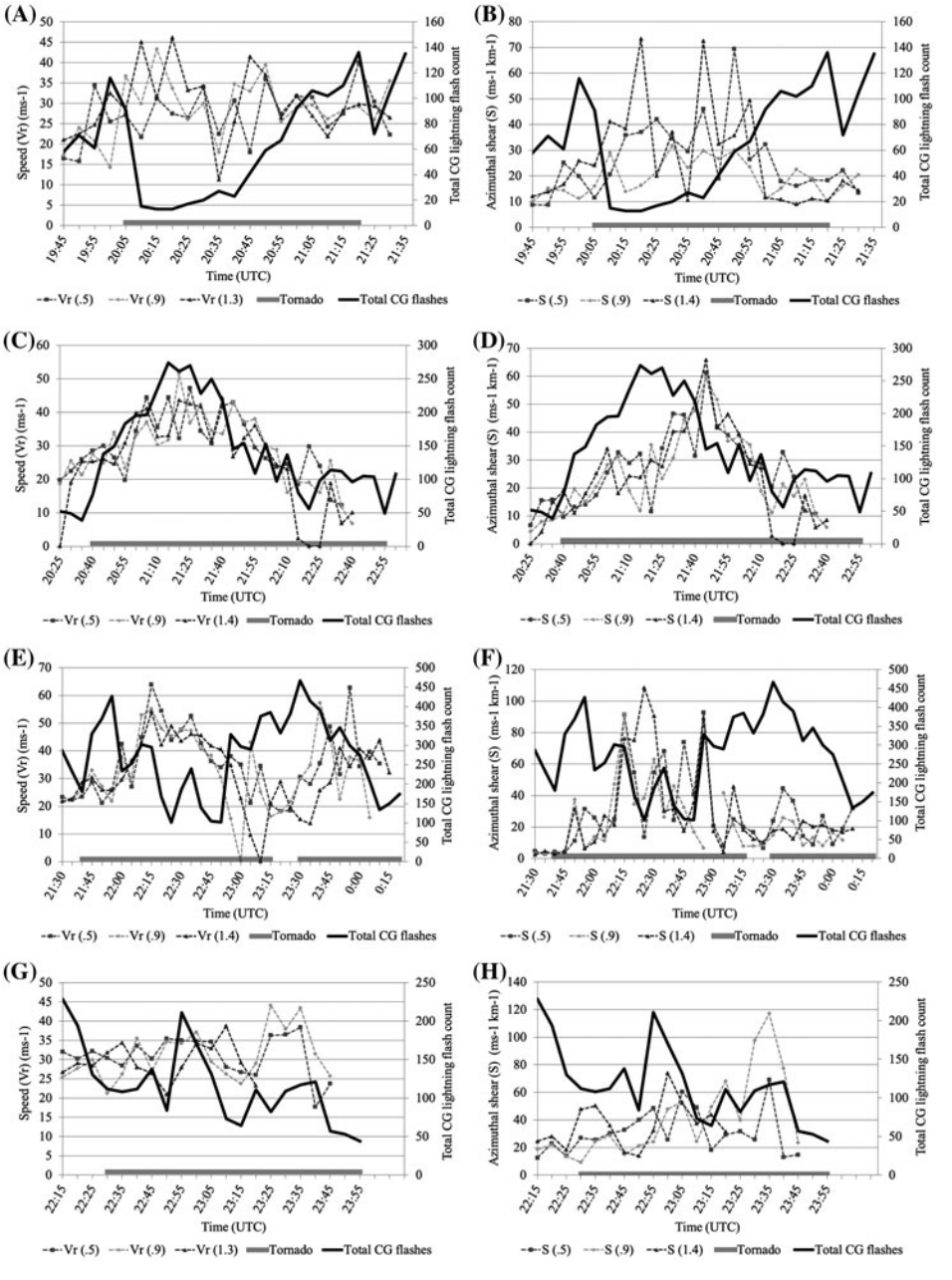

Figure 6. Left column: Rotational velocity (V_r) and total CG flashes.
Notes: Solid black line represents the total CG flashes; darker gray line with the square marker illustrates the rotational velocity at radar elevation angle 0.5°; light gray line with the diamond marker indicates the rotational velocity at radar elevation angle 0.9°; gray line with the triangle marker represents the rotational velocity at radar elevation angle 1.3°/1.4°. Right column: As in the left column except for azimuthal shear and total CG flashes. Tornado events A-1 (panel A and B); C-2 (panel C and D); D-2 (panel E and F); E-1 (panel G and H).

Table 5. Significance testing using a piecewise linear regression and spline regression model test with known knot locations. A ✓ mark indicates a statistically significant lightning jump prior to tornadogenesis utilizing the five-minute binning scheme; an X represents no statistically significant lightning jump prior to tornadogenesis utilizing the five-min binning scheme.

			Confidence interval		
Tornado event	t	P	90%	95%	99%
A-1	−5.639	0.000	✓	✓	✓
B-1	1.273	0.214	X	X	X
C-1	−1.213	0.271	X	X	X
C-2	4.535	0.000	✓	✓	✓
C-3	1.097	0.305	X	X	X
C-4	−0.710	0.496	X	X	X
D-1	0.722	0.478	X	X	X
D-2	2.783	0.015	✓	✓	X
E-1	0.850	0.406	X	X	X
F-1	−0.849	0.401	X	X	X
G-1	2.575	0.018	✓	✓	X

influenced storm polarity characteristics. Storms that typically experience a polarity shift have a tendency to propagate from a region of strong θ_e, experience weakening updrafts, and are no longer able to support the mass of hydrometeors and ice aloft (cf. figure 9 in Smith et al., 2000). This liquid water and ice fallout often results in a polarity reversal (Smith et al., 2000). All storms examined in this study initiated downstream and moved adjacent to the surface θ_e axis. Moreover, none experienced rapid updraft intensification due to a sudden increase in buoyancy of low-level inflow air or abrupt precipitation fallout that could have led to a CG lightning polarity shift (Smith et al., 2000).

In comparison to the results found in previous studies (e.g., Carey et al., 2003; Schultz et al., 2009; Seimon, 1993), the lightning–tornado relationships in the extreme storms examined in this study were inconsistent and/or conflicting. This finding suggests that storm-specific lightning production variables, such as updraft strength, hydrometeor content, FL heights, and WCD, may vary widely across spatial and environmental spaces, leading to differences in total CG flash rates in individual storms.

Lightning and low-level mesocyclone intensity

A storm's updraft is a key factor in determining total lightning activity (MacGorman et al., 1989; Ziegler & MacGorman, 1994). The relationship between lightning flash rates and updraft intensity provides valuable information on a storm's internal charge and dynamical processes. Past studies have examined the relationship among low-level mesocyclone intensity, CG lightning flash rates, as well as IC lightning flash rates and have found that, as the low-level mesocyclone intensifies, the separation between upper charge regions and lower charge regions of the storm increases while CG lightning flash rates decrease (MacGorman et al., 1989; Ziegler & MacGorman 1994). Evidence of this relationship is outlined in MacGorman et al. (1989) where it was established that CG lightning flash rates were negatively correlated with cyclonic shear at the

low- and mid-levels of a storm (1.5 and 6 km). Accordingly, assessing the strength of the negative correlation between CG lightning flash rate and low-level mesocyclone intensity could provide insight into the lightning flash rate–tornadogenesis relationship during the 27–28 April 2011 event.

An assessment of tornado events A-1, C-2, D-2, and E-1 revealed that the association between low-level mesocyclone strength and the total CG lightning flash rate was diverse and variable. Statistical tests were applied to examine further the relationship between azimuthal (rotational) shear total CG lightning flash rates. Correlation coefficient values of −1.0 to −0.5 are argued to be of high strength −0.5 to −0.3 of moderate strength, and −0.3 to −0.1 of weak strength, values greater than −0.1 are indicative of little to no linear relationship between the two variables examined. All tornado events assessed (A-1, C-2, D-2, E-1) were expected to have a negative correlation (r value equal to −1.0 to −0.01) between rotational velocity or azimuthal shear and total CG lightning flash rate.

Tornado event A-1 (Smithville, MS) illustrated a negatively correlated relationship of moderate strength between azimuthal shear and total CG lightning flash rate, tornado event D-2 exemplified a negatively correlated relationship of moderate-to-high strength between rotational velocity and total CG flash rate, and tornado event E-1 had a negatively correlated relationship of moderate strength between azimuthal shear (0.9° elevation angle) and total CG flash rate (Table 6; Figure 6). Tornado event C-2 did not contain a statistically significant *negative* correlation between rotational velocity or azimuthal shear and total CG lightning flash rate using the one-tailed t-test (Table 6; Figure 6).

Results suggest that the intensification or weakening of the low-level mesocyclone is one of many dynamical processes that influence a supercell's internal charge structure that can affect the overall lightning production within the storm. These dynamical processes include precipitation development within the supercell updraft and downdraft regions (Bruning et al., 2010; MacGorman et al., 2005; Stolzenburg, Rust, & Marshall,

Table 6. Tornado events A-1, C-2, D-2, and E-1 regression analysis (R^2), Pearson's product-moment correlation (r), significance testing with the t-distribution (t-calc; one-tailed; $\alpha = 0.05$) between total CG lightning flashes and rotational velocity (V_r)/azimuthal (rotational) shear (S) by Doppler radar scan elevation angle; values in bold font represent *moderate* correlation strength; values italicized illustrate significant correlation values.

Tornado event	Statistic	V_r (0.5)	V_r (0.9)	V_r (1.4)	S (0.5)	S (0.9)	S (1.4)
A-1	R^2	0.000	0.037	0.094	0.233	0.158	0.343
	r	−0.018	−0.194	−0.307	*−0.482*	*−0.397*	*−0.586*
	Sig. test	−0.079	−0.883	−1.441	*−2.462*	*−1.934*	*−3.232*
C-2	R^2	0.404	0.394	0.436	0.102	0.094	0.120
	r	0.635	0.628	0.660	0.320	0.307	0.346
	Sig. test	4.275	4.270	4.570	1.752	1.706	1.952
D-2	R^2	0.240	0.234	0.425	0.035	0.062	0.120
	r	*−0.489*	*−0.483*	*−0.652*	−0.186	−0.249	*−0.346*
	Sig. test	*−3.125*	*−2.974*	*−4.787*	−1.054	−1.382	*−2.052*
E-1	R^2	0.052	0.039	0.003	0.037	0.257	0.004
	r	0.228	−0.198	0.053	−0.192	*−0.507*	−0.064
	Sig. test	0.968	−0.834	0.184	−0.805	*−2.427*	−0.224

1998; Weins, Rutledge, & Tessendorf, 2005), hydrometeor type (Bringi et al., 1997; Goodman, Buechler, Wright, & Rust, 1988; MacGorman et al., 2005; Weins et al., 2005; Williams, Zhang, & Rydock, 1991), hydrometeor fall speeds (Gilmore & Wicker, 2002), and potential influence of lofted debris (Winn, Hunyady, & Aulich, 2000).

While the relationship between CG lightning flash rates and low-level mesocyclone intensity is an indicator of a storm's internal physical and dynamical processes, an increase in total lightning flash rates (IC plus CG) during a time of low-level mesocyclone intensification is principally due to an increase in IC lightning flashes (MacGorman et al., 1989). Thus, the CG lightning flash rate and low-level mesocyclone relationship provides little insight into the lightning flash rate and tornadogenesis connection.

Discussion and conclusions

This study examined the CG lightning–tornado relationship for a set of supercells that occurred during the 27–28 April 2011 United States tornado outbreak. While past research has explored the lightning and severe weather hazard connection, no investigation has observed the lightning–tornado relationship for such a violent severe weather event. Moreover, this research analyzed the CG lightning characteristics of multiple, long-lived, tornadic supercells that formed in a similar kinematic and thermodynamic environment.

Results on the CG lightning–tornado relationship indicate that only 3 of the 11 tornado events demonstrated a local maximum in total CG lightning flash rate prior to tornadogenesis *and* a local minimum in total CG lightning flash rate coincident with tornadogenesis utilizing the five-min binning scheme (Table 4). Seven of eleven tornadic events exemplified an increase in total CG lightning flash rate in the 5 min prior to or concurrent with tornadolysis (Table 4).

An examination of the low-level mesocyclone intensity in relation to total CG lightning flash rate led to inconsistent results, suggesting that that low-level mesocyclone strengthening (weakening) is only one of many potential dynamical processes that influence a storm's internal charge structure and subsequent CG lightning flash rates (Bringi et al., 1997; Gilmore & Wicker 2002; Goodman et al., 1988; Weins et al., 2005; Williams et al., 1991). Like MacGorman et al. (1989), we surmise that IC lightning flashes are mainly responsible for the increase (i.e., lightning jump) during a time of low-level mesocyclone intensification, and that the CG lightning flash rate and low-level mesocyclone relationship represents a much weaker depiction of total lightning flash activity in relation to tornadogenesis. Overall, results illustrate that an increase in total CG lightning flash rates in the moments prior to tornadogenesis was not evident in a majority of storms. The inconsistent storm-to-storm results found in this particular case suggest that more research is required to determine the efficacy of the lightning–tornado relationship in nowcasting operations.

Objective analyses of the relationship between CG lightning flash rate and tornadogenesis revealed that employing CG lightning flashes as a sole metric was not necessarily a robust indicator of lightning jumps prior to tornadogenesis (Table 5). Though CG lightning flash rates do provide a proportional indicator of total lightning activity, it is not sufficient to determine whether or not a statistically significant lightning jump has occurred prior to tornadogenesis. Similar to those of Schultz et al. (2009), our results suggests that when assessing the strength of the lightning jump signal, total lightning flash data, if available, should be employed as they provide a more complete representation (i.e., possible stronger signal) of the lightning–tornado relationship.

When examining the lightning–tornado relationship in the future, research should focus on the spatial aspects, as opposed to magnitude characteristics, of total CG lightning flashes in relation to storm morphology and structure. This spatial analysis should be conducted with a three-dimensional and time-evolving approach to comprehend fully the total lightning flash and storm morphology relationship, which will improve overall understanding of charge formation and lightning production as it relates to updraft size, location, and intensity. The use of satellite-derived total lightning flash detection (IC and CG) as opposed to solely ground-based sensor CG flash detection could improve the overall accuracy and understanding of the lightning and severe thunderstorm hazard relationship (Hodanish et al., 2013; Schultz et al., 2011) and provide a more complete depiction of lightning activity within a thunderstorm. Future research should also increase the sample size of storms examined, with the focus on storms that form in similar kinematic and thermodynamic environments. Increasing the sample size of storms assessed will lead to a more comprehensive understanding of lightning–tornado relationships and allow for increased confidence of utilizing the relationship as a forecasting tool. While the manual lasso method best captured the CG lightning flashes associated with a storm of particular interest in this particular study, future studies should incorporate radar-based cell identification algorithms such as ETITAN (Han et al., 2009) in cases where the storm sample size examined is greater. The implication is that an objective storm-tracking algorithm would eliminate the subjective, user bias that can ultimately impact lightning–tornado relationship findings. Overall, future research needs to put forth an objective, comprehensive, and collaborative effort in order to understand better the lightning–tornado relationship. Only then will the lightning flash rate and tornado relationship become a useful tool for operational forecasters and modelers.

Acknowledgments

We would like to thank those anonymous reviewers who provided useful feedback, suggestions, and comments. We would also like to thank Drs. David Changnon and Andrew Krmenec (NIU) for providing comments and suggestions on early versions of this manuscript, as well as ideas and guidance throughout the entire research process. We thank Donnie Eldridge (Vaisala), Ron Holle (Vaisala), Kevin Laws (NWS/NOAA), Wendell Nuss (Department of Meteorology, Naval Postgraduate School, Monterey, California), Steve Weiss (SPC/NOAA), and Ray Wolf (NWS/NOAA) who provided helpful recommendations, comments, and references for this research. Lastly, we would like to acknowledge the NIU William Morris Davis Fund for Graduate Research which allowed for the purchase of the NLDN lightning data.

References

Atkins, N. T., Bouchard, C. S., Przybylinski, R. W., Trapp, R. J., & Schmocker, G. (2005). Damaging surface wind mechanisms within the 10 June 2003 Saint Louis bow echo during BAMEX. *Monthly Weather Review, 133*, 2275–2296.

Bentley, M. L., & Stallins, J. A. (2005). Climatology of cloud-to-ground lightning in Georgia, USA, 1992–2003. *International Journal of Climatology, 25*, 1979–1996.

Bentley, M. L., Stallins, J. A., & Ashley, W. S. (2012). Synoptic environments favourable for urban convection in Atlanta, Georgia. *International Journal of Climatology, 32*, 1287–1294.

Bluestein, H. B., & MacGorman, D. R. (1998). Evolution of cloud-to-ground lightning characteristics and storm structure in the Spearman, Texas, tornadic supercells of 31 May 1990. *Monthly Weather Review, 126*, 1451–1467.

Bringi, V. N., Knupp, K. R., Detwiler, A., Liu, L., Caylor, I. J., & Black, R. A. (1997). Evolution of a Florida thunderstorm during the convection and precipitation/electrification experiment: The case of 9 August 1991. *Monthly Weather Review, 125*, 2131–2160.

Brooks, H. E., Doswell, C. A., III, & Wilhelmson, R. B. (1994). The role of midtropospheric winds in the evolution and maintenance of low-level mesocyclones. *Monthly Weather Review, 122*, 126–136.

Bruning, E. C., Rust, W. D., MacGorman, D. R., Biggerstaff, M. I., & Schuur, T. J. (2010). Formation of charge structures in a supercell. *Monthly Weather Review, 138*, 3740–3761.

Carcione, B. C., & Stano, G. T. (2012). *An analysis of operational total lightning data during long-track tornadoes*. In Proceedings of 5th International Lightning Meteorology Conference, Broomfield, CO.

Carey, L. D., & Buffalo, K. M. (2007). Environmental control of cloud-to-ground lightning polarity in severe storms. *Monthly Weather Review, 135*, 1327–1353.

Carey, W. A., Petersen, R. A., & Rutledge, S. A. (2003). Evolution of cloud-to-ground lightning and storm structure in the Spencer, South Dakota, Tornadic Supercell of 30 May 1998. *Monthly Weather Review, 131*, 1811–1831.

Carey, W. A., & Rutledge, S. A. (1998). Electrical and multiparameter radar observations of a severe hailstorm. *Journal of Geophysical Research, 103*, 13979–14000.

Changnon, S. A. (1992). Temporal and spatial relations between hail and lightning. *Journal of Applied Meteorology, 31*, 587–604.

Coleman, T. A., Knupp, K., & Murphy, T. (2012). *The dynamics and morphology of two long-track tornadic supercells on 27 April 2011*. In Proceedings of 92 American Meteorological Society Annual Meeting, New Orleans, LA.

Cope, A. M. (2006). *Toward better use of lightning data in operational forecasting*. In Proceedings of 2nd Conference on Meteorological Applications of Lightning Data, Atlanta, GA.

Cummins, K. L., & Murphy, M. J. (2009). An overview of lightning locating systems: History, techniques, and data uses, with an in-depth look at the US NLDN. *IEEE Transactions on Electromagnetic Compatibility, 51*, 499–518.

Cummins, K. L., Murphy, M. J., Bardo, E. A., Hiscox, W. L., Pyle, R. B., & Pifer, A. E. (1998). A combined TOA/MDF technology upgrade of the US National Lightning Detection Network. *Journal of Geophysical Research, 103*, 9035–9044.

Deierling, W., & Petersen, W. A. (2008). Total lightning activity as an indicator of updraft characteristics. *Journal of Geophysical Research, 113*, 1–11.

Dixon, M., & Wiener, G. (1993). TITAN: Thunderstorm identification, Tracking, analysis, and nowcasting – A radar-based methodology. *Journal of Atmospheric and Oceanic Technology, 10*, 785–797.

Falconer, P. D. (1984). A radar-based climatology of thunderstorm days across New York state. *Journal of Climate and Applied Meteorology, 23*, 1115–1120.

Gilmore, M. S., & Wicker, L. J. (2002). Influences of the local environment on supercell cloud-to-ground lightning, radar characteristics, and severe weather on 2 June 1995. *Monthly Weather Review, 130*, 2349–2372.

Glickman, T. S. (2000). *Glossary of meteorology* (2nd ed.). Boston: American Meteorological Society.

Goodman, S. J., Buechler, D. E., Wright, P. D., & Rust, W. D. (1988). Lightning and precipitation history of a microburst-producing storm. *Geophysical Research Letters, 15*, 1185–1188.

Han, L., Fu, S., Zhao, L., Zheng, Y., Wang, H., & Lin, Y. (2009). 3D convective storm identification, tracking, and forecasting – An enhanced TITAN algorithm. *Journal of Atmospheric and Oceanic Technology, 26*, 719–732.

Harlin, J. D., Hamlin, T. D., Krehbiel, P. R., Thomas, R. J., Rison, W., & Shown, D. (2000). LMA observations of tornadic storms during STEPS 2000. *Eos, Transactions of the AGU, 81*, A52C–25.

Hodanish, S. J., Williams, E., & Boldi, B. (2013). Early history of using total lightning data at NWS Melbourne, Florida. *Electronic Journal of Severe Storms Meteorology, 8*(6), 1–26.

Johnson, J. T., MacKeen, P. L., Witt, A., Mitchell, E. D., Stumpf, G. J., Eilts, M. D., & Thomas, K. W. (1998). The storm cell identification and tracking algorithm: An enhanced WSR-88D algorithm. *Weather and Forecasting, 13*, 263–276.

Kane, R. J. (1991). Correlating lightning to severe local storms in the northeastern United States. *Weather and Forecasting, 6*, 3–12.

Knapp, D. I. (1994). Using cloud-to-ground lightning data to identify tornadic thunderstorm signatures and nowcast severe weather. *National Weather Digest, 19*, 35–42.

Knupp, K. R., Murphy, T. A., Coleman, T. A., Wade, R. A., Mullins, S. A., Schultz, C. J., Schultz, E. V., Carey, L., & Sherrer, A. (2013). Meteorological overview of the devastating 27 April 2011 Tornado outbreak. *Bulletin of the American Meteorological Society*. doi:http://dx.doi.org/10.1175/BAMS-D-11-00229.1

Knupp, K. R., Paech, S., & Goodman, S. (2003). Variations in cloud-to-ground lightning characteristics among three adjacent tornadic supercell storms over the Tennessee valley region. *Monthly Weather Review, 131*, 172–188.

Kotroni, V., & Lagouvardos, K. (2008). Lightning occurrence in relation with elevation, terrain slope, and vegetation cover in the Mediterranean. *Journal of Geophysical Research, 113*, D21118. doi:10.1029/2008JD010605

Kufa, N., & Snow, R. (2006). *Lightning: Meteorology's new tool*. In Proceedings of 2nd Conference on Meteorological Applications of Lightning Data, Atlanta, GA.

Kuhlman, K. M., Ziegler, C. L., Mansell, E. R., MacGorman, D. R., & Straka, J. M. (2006). Numerically simulated electrification and lightning of the 29 June 2000 STEPS supercell storm. *Monthly Weather Review, 134*, 2734–2757.

Lang, T. J., & Rutledge, S. A. (2002). Relationships between convective storm kinematics, precipitation, and lightning. *Monthly Weather Review, 130*, 2492–2506.

Lang, T. J., & Rutledge, S. A. (2005). *One severe storm with two distinct electrical regimes during its lifetime: Implications for nowcasting severe weather with lightning data*. In Proceedings of 1st Conference of Meteorological Applications of Lightning Data, San Diego, CA.

MacGorman, D. R. (1993). Lightning in tornadic storms: A review. The tornado: Its structure, dynamics, prediction, and hazards. *American Geophysical Union, 79*, 173–182.

MacGorman, D. R., & Burgess, D. W. (1994). Positive cloud-to-ground lightning in tornadic storms and hailstorms. *Monthly Weather Review, 122*, 1671–1697.

MacGorman, D. R., Burgess, D. W., Mazur, V., Rust, W. D., Taylor, W. L., & Johnson, B. C. (1989). Lightning rates relative to tornadic storm evolution on 22 May 1981. *Journal of the Atmospheric Sciences, 46*, 221–251.

MacGorman, D. R., Rust, W. D., Krehbiel, P. R., Rison, W., Bruning, E. C., & Wiens, K. (2005). The electrical structure of two supercell storms during STEPS. *Monthly Weather Review, 133*, 2583–2607.

Mäkelä, A. R., Pekka, D. M., & Shultz, D. (2011). The daily cloud-to-ground lightning flash density in the contiguous United States and Finland. *Monthly Weather Review, 139*, 1323–1337.

Marsh, L. C., & Cormier, D. R. (2002). Spline knot locations known in advance. *Series: Quantitative applications in the social sciences, spline regression models* (pp. 3–5). Beverly Hills, CA: Sage.

Martinez, M., & Schroder, J. L. (2004). *Lightning signatures in convective systems in the high plains*. In Proceedings of 22nd conference on Severe and Local Storms, Hyannis, MA.

McCaul, E. W., Jr, Buechler, D. E., Hodanish, S., & Goodman, S. J. (2002). The Almena, Kansas, tornadic storm of 3 June 1999: A long-lived supercell with very little cloud-to-ground lightning. *Monthly Weather Review, 130*, 407–415.

McDonald, M., McCarthy, P. J., & Patrick, D. (2006). *Anomalous lightning behavior in northern plains tornadic supercell*. In Proceedings of 23rd conference for Severe and Local Storms, St. Louis, MO.

McDowall, D., McCleary, R., Meidinger, E. E., & Hay, R. A., Jr. (1980). An abrupt, permanent impact. *Series: Quantitative applications in the social sciences, Interrupted time series analysis* (pp. 67–74). Beverly Hills, CA: Sage.

McKinney, C. M., Carey, L. D., & Patrick, G. R. (2009). Total lightning observations of supercells over north central Texas. *Electronic Journal of Severe Storms Meteorology, 4*(2), 1–25.

Murphy, M. J., & Demetriades, N. W. (2005). *An analysis of lightning holes in a DFW supercell storm using total lightning and radar information*. In Proceedings of, 85th Annual AMS meeting 2.3 Conference, San Diego, CA.

National Oceanic Atmospheric Administration (NOAA), National Weather Service (NWS). (2011). *The historic tornadoes of April 2011*. Silver Spring, MD: National Oceanic and Atmospheric Administration. National Weather Service.

Orville, R. E. (2008). Development of the national lightning detection network. *Bulletin of the American Meteorological Society, 89*, 180–190.

Orville, R. E., Huffines, G. R., Burrows, W. R., & Cummins, K. L. (2010). The North America lightning detection network (NADLN): Analysis of flash data 2001–2009. *Monthly Weather Review, 139*, 1305–1322.

Parker, M. D., & Knievel, J. C. (2005). Do meteorologists suppress thunderstorms? Radar-derived statistics and the behavior of moist convection. *Bulletin of the American Meteorological Society, 86*, 341–358.

Perez, A. H., Wicker, L. J., & Orville, R. E. (1997). Characteristics of cloud-to-ground lightning associated with violent tornadoes. *Weather and Forecasting, 12*, 428–437.

Rasmussen, E. N., & Blanchard, D. O. (1998). A baseline climatology of sounding-derived supercell and tornado forecast parameters. *Weather and Forecasting, 13*, 1148–1164.

Rickenbach, T. M., & Rutledge, S. A. (1998). Convection in TOGA COARE: Horizontal scale, morphology, and rainfall production. *Journal of the Atmospheric Sciences, 55*, 2715–2729.

Rosenfeld, D., & Woodley, W. L. (2003). Spaceborne inferences of cloud microstructure and precipitation processes: Synthesis, insights, and implications. *Meteorological Monographs,* 51, 59–80 (American Meteorologial Society).

Saunders, C. P. R. (1994). Thunderstorm electrification laboratory experiments and charging mechanisms. *Journal of Geophysical Research, 99*, 10773–10779.

Schultz, C. J., Petersen, W. A., & Carey, L. D. (2009). Preliminary development and evaluation of lightning jump algorithms for the real-time detection of severe weather. *Journal of Applied Meteorology and Climatology, 48*, 2543–2563.

Schultz, C. J., Petersen, W. A., & Carey, L. D. (2011). Lightning and severe weather: A comparison between total and cloud-to-ground lightning trends. *Weather and Forecasting, 26*, 744–755.

Seimon, A. (1993). Anomalous cloud-to-ground lightning in an F-5 tornado producing thunderstorm on 28 August 1990. *Bulletin of the American Meteorological Society, 74*, 189–203.

Shafer, M. A., MacGorman, D. R., & Carr, F. H. (2000). Cloud-to-ground lightning throughout the lifetime of a severe storm system in Oklahoma. *Monthly Weather Review, 128*, 1798–1816.

Smith, S. B., LaDue, J. G., & MacGorman, D. R. (2000). The relationship between cloud-to-ground lightning polarity and surface equivalent potential temperature during three tornadic outbreaks. *Monthly Weather Review, 128*, 3320–3328.

Steiger, S. M., Orville, R. E., Murphy, M. J., & Demetriades, N. W. (2005). *Total lightning and radar characteristics of supercells*: Insights on electrification and severe weather forecasting. In Proceedings of 85th Annual AMS meeting 2.3 Conference, San Diego, CA.

Stolzenburg, M., Rust, W. D., & Marshall, T. C. (1998). Electrical structure in thunderstorm convective regions: 3. Synthesis. *Journal of Geophysical Research, 103*, 14097–14108.

Stumpf, G. J., Witt, A. E., M., DeWayne, S. L., Phillip, Johnson, J. T., Eilts, M. D., Thomas, K. W., & Burgess, D. W. (1998). The national severe storms laboratory mesocyclone detection algorithm for the WSR-88D. *Weather and Forecasting, 13*, 304–326.

Wacker, R. S., & Orville, R. E. (1999). Changes in measured lightning flash count and return stroke peak current after the 1994 US national lightning detection network upgrade: 1. Observations. *Journal of Geophysical Research, 104*, 2151–2157.

Weins, K. C., Rutledge, S. A., & Tessendorf, S. A. (2005). The 29 June 2000 supercell observed during STEPS. Part II: Lightning and charge structure. *Journal of the Atmospheric Sciences, 62*, 4151–4177.

Williams, E. R., Zhang, R., & Rydock, J. (1991). Mixed-phase microphysics and cloud electrification. *Journal of the Atmospheric Sciences, 48*, 2195–2203.

Winn, W. P., Hunyady, S. J., & Aulich, G. D. (2000). Electric field at the ground in a large tornado. *Journal of Geophysical Research, 105*(D15), 20145–20153.

Wolf, R. (2006). *A preliminary assessment of the environmental and radar characteristics of tornadic and non-tornadic mesovortices associated with QLCSs*. In Proceedings of 23rd Conference Severe Local Storms, St. Louis, Missouri.

Ziegler, C. L., & MacGorman, D. R. (1994). Observed lightning morphology relative to modeled space charge and electric field distributions in a tornadic storm. *Journal of the Atmospheric Sciences, 51*, 833–851.